

## Tomographic Studies of the sQGP at RHIC

Wolf G. Holzmann<sup>1</sup> for the PHENIX Collaboration

<sup>1</sup> Department of Chemistry, State University of New York at Stony Brook,  
Stony Brook, New York 11794-3400, USA

**Abstract.** Azimuthal correlation functions are used to study jet- and di-jet properties as a function of centrality in Au+Au collisions at  $\sqrt{s_{NN}}=200$  GeV. Utilizing a novel technique to decompose the correlation function into a (di-)jet and an underlying event, the jet-pair distribution is extracted and compared to similar results for d+Au collisions obtained at the same collision energy. A striking similarity is observed between the widths and associated yields of the (di-)jet distributions for d+Au and peripheral Au+Au collisions. By contrast, the distributions for mid-central Au+Au collisions indicate an increase in the di-jet yield with centrality, and a very broad away-side jet having a possible minimum at  $\Delta\phi \approx \pi$ . These features point to significant medium induced modification to the away-side jet and are compatible with recent predictions of jet-induced “conical flow”.

*Keywords:* RHIC, PHENIX, QGP, sQGP, correlations, jets, conical flow, mach cones, Au+Au, d+Au

*PACS:* specifications see, e.g. <http://www.aip.org/pacs/>

### 1. Introduction

Reactions between Au ions at the Relativistic Heavy Ion Collider (RHIC), indicate the creation of a fireball of nuclear matter having energy density well above that required for a de-confined phase of quarks and gluons (QGP) [ 1, 2]. The decay of this matter results in large azimuthal anisotropies in the particle emission patterns, suggesting early thermalization and the development of substantial pressure gradients which drive the dynamical evolution of the system [ 3, 4, 5, 6, 7, 8]. Hydrodynamic evolution of the fireball is further corroborated by the observation of strong radial flow [ 9] and first hints of a long-range emitting source from a recent Imaging analysis [ 10, 11]. Strong indications for hydrodynamic evolution of the emitting system implies the production of strongly interacting high energy density matter in energetic RHIC collisions [ 4, 6, 8]. Indeed, this matter has been ob-

served to strongly suppress the yield of hadrons with large transverse momenta [ 12, 13, 14, 15] and to suppress the away-side jet in central Au+Au collisions [ 16]. It is believed that this suppression results from energy loss of hard-scattered partons traversing the high energy density matter prior to the formation of hadrons [ 17, 18, 19, 20, 21, 22].

An important open question of great current interest is the influence of the parton-medium interactions on jet properties. Such an influence is of paramount importance if one wants to use jets as a probe of the properties of strongly interacting high energy density matter. Several recent works have outlined a possible influence of the coupling between jets and a strongly interacting medium [ 23, 24, 25, 26, 27, 28, 29, 30, 31]. A particularly important proposal is the conjecture that the energy deposited in the medium could lead to the creation of a shock wave around the propagating parton, thereby creating “conical flow” or “bow waves” analogous to a sonic boom in a fluid[ 27, 28, 29, 30]. The experimental observation of such conical flow could serve to pin down the sound speed in the nuclear matter created at RHIC.

In order to probe the influence of possible parton-medium interactions on jet properties, we use azimuthal angular correlation functions to investigate jet topologies and yields in d+Au and Au+Au collisions. Here, the operational strategy is that d+Au measurements provide a good baseline for comparison to the Au+Au measurements which are expected to show much stronger modifications to jet properties.

## 2. Data Analysis

The analysis presented in this paper uses Au+Au and d+Au data ( $\sqrt{s_{NN}}=200$  GeV) provided by RHIC in the second and third running periods (2001,2003), respectively. The full PHENIX detector setup is described elsewhere [ 32]. Charged tracks relevant to this analysis were reconstructed in the central arms of PHENIX, each of which covers 90 degrees in azimuth. Tracking was performed via the drift chamber and two layers of multi-wire proportional chambers with pad readout (PC1,PC3)[ 32]. A combinatorial Hough transform in the track bend plane was used for pattern recognition[ 33]. Most conversions, albedo and decays were rejected by requiring a confirmation hit within a  $2\sigma$  matching window in the PC3. Collision centrality was determined via cuts in the space of BBC versus ZDC analog response [ 34].

The correlation function in relative azimuthal angle between particle pairs,  $\Delta\phi = (\phi_1 - \phi_2)$ , is defined as the ratio of two distributions

$$C(\Delta\phi) \propto \frac{N_{cor}(\Delta\phi)}{N_{mix}(\Delta\phi)}. \quad (1)$$

The foreground distribution  $N_{cor}$ , measures coincident particle pairs from the same event by pairing particles from a high- $p_T$  “trigger” bin ( $2.5 < p_T < 4.0$  GeV/c, hereafter labeled A) with associated particles from a lower  $p_T$  selection ( $1.0 < p_T <$

2.5 GeV/c, hereafter labeled B). The background distribution  $N_{mix}$ , is generated in an analogous way by mixing particle pairs from different events within the same multiplicity and vertex class. The Azimuthal acceptance and detector efficiency effects cancel in the ratio of foreground to background distributions and the correlation function yields the probability distribution for detecting correlated particle pairs per event within the PHENIX pseudorapidity acceptance ( $|\eta| < 0.35$ ). Fig. 1

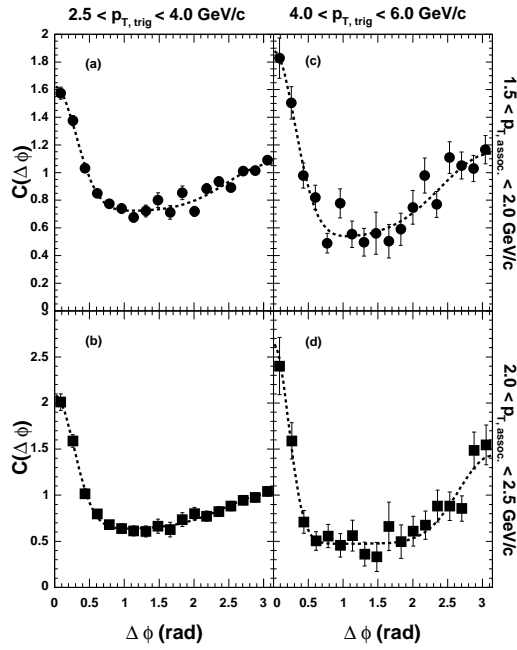


**Fig. 1.** d+Au correlation functions  $C(\Delta\phi)$  for several  $p_T$  selections as indicated. The centrality selection is 0-80%. The dashed line represents a double gaussian fit to the data.

shows d+Au correlation functions for two different trigger and associated  $p_T$  selections as indicated. The centrality selection is 0-80%. The dashed line represents a double Gaussian fit to the data. These d+Au correlation functions exhibit a shape reminiscent of what one would expect from di-jet fragmentation. That is, a relatively narrow near-side peak centered at  $\Delta\phi = 0$  and a somewhat wider away-side peak centered at  $\Delta\phi = \pi$ . Fig. 1 shows that both near-side and away-side peaks narrow and are more pronounced for higher  $p_T$ -selections of trigger and associated

particles, respectively. Such a pattern is expected if (di-)jet fragmentation is the dominant particle production mechanism at high transverse momenta. It is noteworthy that the widths (of near- and away-side jets) and the yields obtained from d+Au correlation functions are rather similar to those obtained from p+p collisions. Consequently, we ascribe all correlation in d+Au collisions to jets.

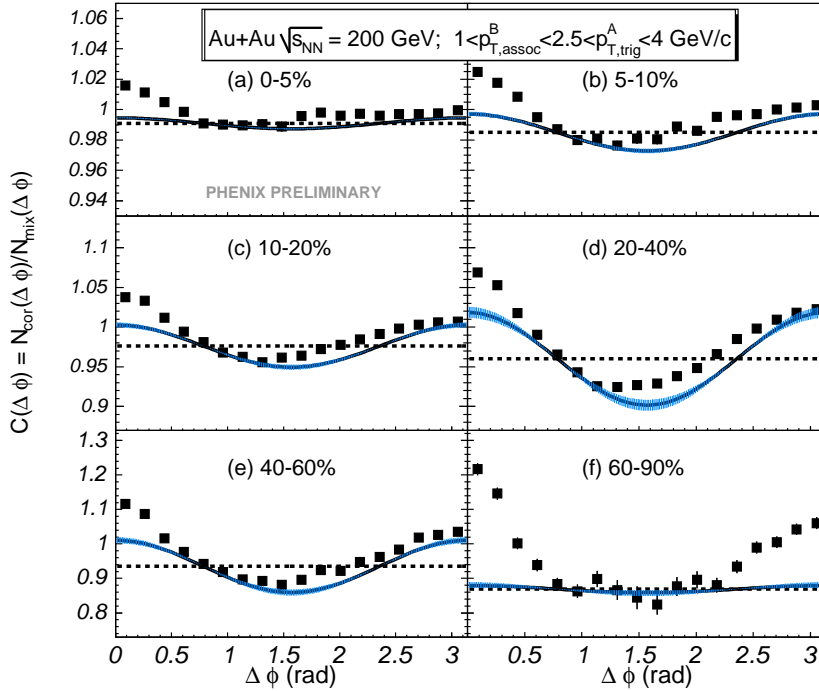


**Fig. 2.** Correlation functions  $C(\Delta\phi)$ , generated for trigger particles in  $2.5 \text{ GeV}/c < p_T^A < 4.0 \text{ GeV}/c$  and associated particles in  $1.0 \text{ GeV}/c < p_T^B < 2.5 \text{ GeV}/c$ . The bands show the harmonic contribution within the systematic uncertainty. The dotted lines indicate the value of  $a_o$  (see text).

The d+Au correlation functions (cf. Fig. 1) are to be compared to the correlation functions for Au+Au data shown in Fig. 2. The filled squares in the figure show correlation functions for AB charged hadron pairs for several indicated centralities. It is difficult to overlook the striking similarity between the correlation function obtained for the most peripheral collisions (cf. Fig. 2f) and that obtained

for d+Au collisions (cf. Fig. 1). Both correlation functions show the two narrow peaks (located at  $\Delta\phi = 0$  and  $\Delta\phi = \pi$ ) characteristic of (di-)jet fragmentation. By contrast, the correlation functions for more central Au+Au collisions show strong indications for a harmonic component and hints for a broad away-side jet i.e. the correlation functions show a minimum below  $\Delta\phi = \pi/2$ . Such a shift away from the minimum expected for harmonic contributions, can only come about if the away-side jet is significantly broader than that observed in d+Au collisions. An important finding that should be stressed here is that the observed characteristics of all of the Au+Au correlation functions can be fully accounted for via two contributions to the correlation function: (i) a (di-)jet and (ii) a harmonic contribution [ 16, 35, 36, 37].

### 3. Decomposition of jet and harmonic contributions

Careful investigation of possible modifications to the di-jet distributions in Au+Au collisions require access to the jet-pair distribution without the blurring effects of the harmonic contributions. Consequently, a reliable procedure for decomposing the measured correlation functions into their (di-)jet and harmonic (or flow) contributions are required. Detailed descriptions of such a procedure are given in Refs. [ 38, 39]. We give here only an outline of the main points.

It can be shown [ 38] that the pair correlations from the combination of flow and jet sources is given by

$$C^{AB}(\Delta\phi) = a_o[C_H^{AB}(\Delta\phi)] + J(\Delta\phi), \quad (2)$$

where  $C_H^{AB}(\Delta\phi)$  is a harmonic function of effective amplitude  $v_2$ ,

$$C_H^{AB}(\Delta\phi) = [1 + 2v_2 \cos 2(\Delta\phi)]; \quad v_2 = (v_2^A \times v_2^B). \quad (3)$$

and  $J(\Delta\phi)$  is the (di-)jet function. No explicit or implicit assumption is required for the functional form of  $J(\Delta\phi)$ . Rearrangement of Eq. 2 gives

$$J(\Delta\phi) = C^{AB}(\Delta\phi) - a_o C_H^{AB}(\Delta\phi). \quad (4)$$

Thus, one only requires knowledge about  $a_o$  and  $v_2$  to evaluate  $J(\Delta\phi)$ . To constrain,  $a_o$  we assume that the (di-)jet function has zero yield at the minimum (ZYAM)  $\Delta\phi_{min}$ , in the jet function, i.e.  $a_o C_H^{AB}(\Delta\phi_{min}) = C^{AB}(\Delta\phi_{min})$ . This fixes the value of  $a_o$ .

The  $v_2$  value reflects the average anisotropy of the particles from both sources, and can be obtained from the single particle distributions relative to the reaction plane  $\psi_R$ . However, this step requires that the reaction plane is itself determined by a procedure essentially free of non-flow effects. This is accomplished in the present analysis by demanding a large (pseudo)rapidity gap ( $\Delta\eta \sim 3 - 3.9$ ) between the reaction plane and the particles correlated with it [ 40, 41]. It is expected that the  $v_2$  values so obtained are much less affected by jet contributions [ 40]. In addition, the reaction plane (at each centrality) and its dispersion correction, and  $v_2^A$  and  $v_2^B$  were

obtained from the same data set used for jet function extraction in order to avoid potential biases. Correction for reaction plane dispersion followed the procedures outlined in Ref. [ 42].

### 3.1. Simulation tests

Prior to applying the decomposition method to PHENIX data, its reliability was thoroughly tested via extensive Monte Carlo simulations [ 39]. These investigations included simulation tests which took account of the  $\phi$  and the  $\eta$  acceptance of PHENIX. Representative results from these Monte Carlo investigations are summarized in Fig. 3. Panel (a) depicts the azimuthal distribution of the simulated reaction products with respect to the event plane. The smooth line is a harmonic fit to the data to extract  $v_2$ . This  $v_2$  determines the amplitude of the harmonic component (dashed line in panel (b)) to be subtracted from the correlation function (filled circles) shown in panel (b). The solid squares in panel (b) shows the ZYAM subtracted jet-pair distribution referenced to  $a_o$ . This distribution is to be compared to the input jet pair distribution (solid line) obtained via tagging of the jet-particles in the simulation. The rather good agreement shown between input and output jet-pair distributions in Fig. 3b serves to confirm the reliability of the method. The method is easily generalized to the case in which trigger particle detection is constrained within a cut angle parallel or perpendicular to the reaction plane [ 39]. Results from simulations in which such constraints have been applied are summarized in panels (c) and (d) of Fig.3. In this case, the harmonic function is determined following the techniques outlined in [ 43]. Here again, panels (c) and (d) clearly indicate that the input jet function is reproduced in detail. It is noteworthy that a wide range of tests for a variety of input jet-pair distributions including those that might be expected from conical flow, were made with equally good recovery of the input jet-pair distributions [ 39].

### 3.2. Decomposition of the measured correlation functions

The solid bands in each panel of Fig. 2 illustrate the application of the ZYAM condition to PHENIX data with the measured values of  $v_2$  ( $v_2 = (v_2^A \times v_2^B)$ ). The dashed lines show the  $a_o$  value obtained for each centrality. Following Eq. 4, the jet-pair distribution is obtained at each centrality via subtraction of the harmonic contribution from the correlation function. It is straightforward to show that the integral of this distribution is related to the average fraction of jet-correlated particle pairs per event and hence the conditional per trigger yield [ 38, 39]. The ratio of the sum of  $J(\Delta\phi)$  and the sum of  $C(\Delta\phi)$  (over all bins in  $\Delta\phi$ ) gives the fraction of jet-correlated particle pairs per event  $PF$ ,

$$PF = \frac{\sum_i J(\Delta\phi_i)}{\sum_i C(\Delta\phi_i)} \quad (5)$$

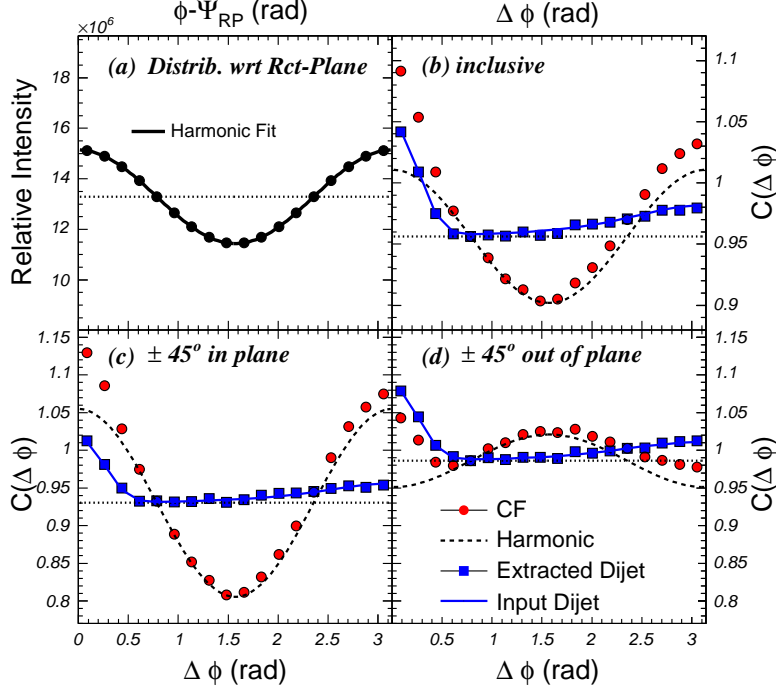


**Fig. 3.** Simulation test of the ZYAM decomposition procedure from [ 39]. (a) simulated azimuthal distribution of particles with respect to the event plane. (b) Simulated correlation function with harmonic component and extracted jet-pair distribution. The solid line represents the input jet-pair distribution (referenced to  $a_o$ ) as obtained from tagging the jet particles in the simulation. (c) and (d) same as (b) but for trigger particles constrained in-plane and out-of-plane respectively (see text).

Subsequent multiplication of this fraction by the average number of detected particle pairs per event  $\langle N_d^{AB} \rangle$ , followed by a division by the product of the detected singles rates  $\langle N_d^A \rangle$ ,  $\langle N_d^B \rangle$ , gives the event averaged jet-pair production in excess of the combinatoric pair production. A final product with the efficiency corrected singles rate  $\langle N_{eff}^B \rangle$ , for bin B, gives the efficiency corrected pairs per trigger or conditional

yield  $CY$  [ 38, 39],

$$CY = PF \times \frac{\langle N_d^{AB} \rangle}{\langle N_d^A \rangle \times \langle N_d^B \rangle} \times \langle N_{eff}^B \rangle. \quad (6)$$

#### 4. Results

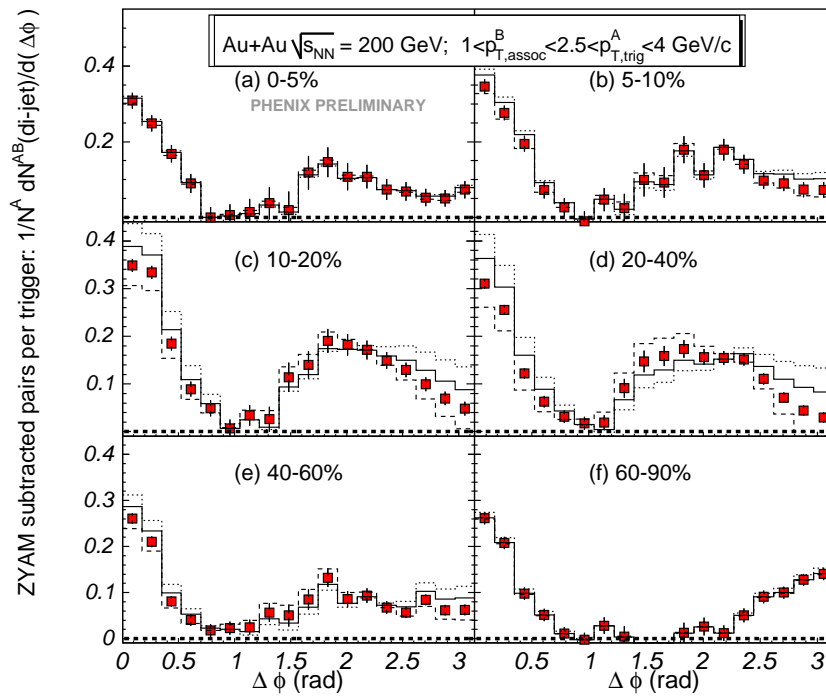


**Fig. 4.** ZYAM-subtracted jet-pair distributions  $1/N_{trig}dN/d(\Delta\phi)$ . The dashed(solid) histograms indicate the distributions resulting from increasing(decreasing)  $v_2 = v_2^A \times v_2^B$  by one interval of the systematic error.

The ZYAM-subtracted conditional yield distributions, normalized to the number of jet-pairs per trigger particle, are shown in Fig. 4. The distribution for the 60-90% peripheral event sample (cf. Fig. 4f) shows the typical (di-)jet shape that is familiar from p+p and d+Au collisions at RHIC. It consists of two distinct peaks,

one narrow near-side peak centered at  $\Delta\phi = 0$  and a broader away-side peak at  $\Delta\phi = \pi$ . It is interesting to trace the evolution of these peaks with collision centrality, as one expects to make increasing amounts of hot and dense matter in the more central collisions. Scanning the mid-central and central jet-pair distributions (Fig. 4a-e), one observes that the near-side peak topology remains essentially unmodified. We attribute this to a possible trigger bias of the near-side jet. However, it should be noted that the near-side yield does show a mild rise with centrality as discussed below. In contrast to the near-side peak, the away-side peaks show indication for strong modifications (both in magnitude and in shape) for all centralities other than the most peripheral event selection. More precisely, in the 0-5%, 5-10% and 40-60% samples, the away-side peak evidences a plateau like shape which is decidedly non-gaussian and much broader in width than that for the 60-90% sample. For the 10-20% and 20-40% samples (Fig. 4c-d), the away-side peak remains broad but also indicates an apparent local minimum at  $\Delta\phi = \pi$  and a maximum at  $\Delta\phi = 2\pi/3$ . This latter pattern is similar to recent predictions of jet-induced "conical flow" [ 27, 28, 29]. It should be pointed out however that these results do not preclude an alternative scenario which conjectures the combined influence of energy loss and the inclination angle of the jet with the flow field [ 26]. Nonetheless, both approaches require relatively strong coupling between jets and the high energy density medium.

The solid (dashed) lines in Fig.4 represent the conditional yield distributions that would result from subtracting out a  $v_2$  product lowered (raised) by one systematic error, respectively. The systematic error on  $v_2$  is dominated by the uncertainty on the reaction plane dispersion. The dotted line indicates the jet-pair distribution resulting from a subtraction with  $v_2$  product lowered by twice the systematic uncertainty. From these curves, one can see that a decrease in  $v_2$  by two intervals of the systematic error can recover the local minimum at  $\Delta\phi = \pi$ . However, the result of a broadened away-side jet remains robust and the away-side jet-shapes remain non-Gaussian. Several studies are currently underway to firm up the mechanism/s responsible for the atypical away-side jet topologies observed in Au+Au collisions.

To better quantify these jet properties, we split the jet-pair distributions into a near-side range,  $0 - \Delta\phi_{min}$  and an away-side range  $\Delta\phi_{min} - \pi$ . The near- and away-side parts of the distribution are then further characterized by their RMS (taken around 0 and  $\pi$ ) and their yield of associated pairs per trigger. These results are summarized in Fig.5 as a function of centrality. For comparison, similar results are included for the 0-20% most central d+Au collisions (open circles) obtained at  $\sqrt{s_{NN}} = 200\text{GeV}$ . The systematic uncertainty in  $v_2$  has been propagated into the systematic errors for yields and RMS values. The systematic error on the yields also accounts for the systematic uncertainty on the single particle reconstruction efficiency.

Fig.5b shows that both the near- and away-side widths for peripheral (60-90%) Au+Au collisions compare well with those obtained for d+Au collisions. This is consistent with the expectation of very little, if any, medium induced modifications to jet-topologies in peripheral Au+Au collisions. An inspection of the centrality de-

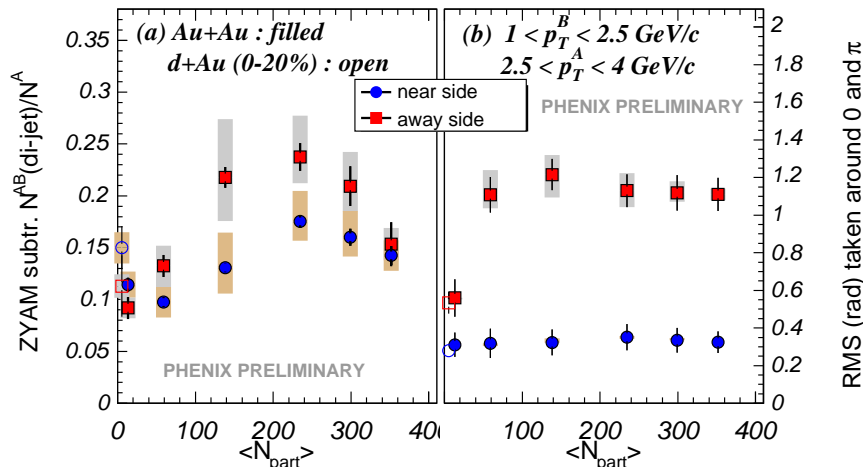


**Fig. 5.** (a) Associated yields for near- and away-side peaks in the jet-induced pair distribution; and (b) Widths (RMS) of the peaks. The open symbols denote results for 0-20% most central d+Au events from a recent PHENIX analysis.

pendence of the near-side RMS shows no apparent change with centrality. On the other hand, the away-side width is significantly broadened for all but the most peripheral event sample, possibly indicating strong modifications to the fragmentation process by the hot nuclear medium. Although the near-side widths are centrality independent, Fig.5a points to a mild increase in the near-side conditional yield from peripheral to central Au+Au collisions, possibly indicating that even the near-side fragmentation process might still be influenced by the medium. The apparent differences in the evolution of near- and away-side jet characteristics could be signaling the contribution of several different mechanisms to jet-modification.

## 5. Conclusions

In summary, we have used a novel correlation function technique to decompose jet correlations from collective long range harmonic correlations (elliptic flow). We find, that the extracted jet-pair distributions show a strong centrality dependent change in shape and associated per-trigger yield, especially for the away-side jet. The jet-pair distributions obtained for peripheral Au+Au collisions are very similar to those obtained for d+Au collisions but the distributions for more central Au+Au collisions are markedly different and are qualitatively consistent with several recent theoretical predictions of possible modification to jet fragmentation by a strongly interacting

medium [ 29, 27, 28, 30, 26]. Further experimental and theoretical studies are clearly required to establish the detailed mechanism/s responsible for the observed jet modification/s and to pin down the properties of the high energy density strongly interacting matter produced in energetic Au+Au collisions at RHIC. Several such studies are currently being pursued with vigor.

## Acknowledgments

I would like to thank the organizers for giving me the opportunity to present these results in such a stimulating and friendly environment. I am deeply grateful to the Nuclear Chemistry Gang at Stony Brook for much more than I have space left to write. Finally, these acknowledgments would not be complete without a big Thank You to the PHENIX collaboration and the RHIC team.

## References

1. K. Adcox et al., submitted to *Nucl. Phys. A*. [nucl-ex/0410003].
2. Z. Fodor and S.D. Katz, *JHEP* **03** (2002) 014.
3. R.A. Lacey, *Nucl. Phys.* **A698** (2002) 559.
4. E.V. Shuryak, (2002) [hep-ph/0405066].
5. A. Taranenko, these proceedings.
6. M. Gyulassy and L. McLerran, *Nucl. Phys.* **A750** (2005) 30.
7. U.W. Heinz, (2005) [nucl-th/0504011]
8. U.W. Heinz, (2005) [nucl-th/0407067]
9. N. Xu and M. Kaneta, *Nucl. Phys.* **A698** (2002) 306.
10. R.A. Lacey, these proceedings.
11. P. Chung et al., *Nucl. Phys.* **A749** (2005) 275c.
12. K. Adcox et al., *Phys. Rev. Lett.* **88**, 022301 (2002).
13. S.S. Adler et al., *Phys. Rev. Lett.* **91**, 072301 (2003).
14. J. Adams et al., *Phys. Rev. Lett.* **91**, 172302 (2003).
15. S.S. Adler et al., *Phys. Rev.* **C69**, 034910 (2004).
16. C. Adler et al., *Phys. Rev. Lett.* **90** 082302 (2003).
17. J.D. Bjorken, (1982) FERMILAB-PUB-82-059-THY.
18. D. A. Appel, *Phys. Rev.* **D33**, 717 (1986).
19. J. P. Blaizot, et al. *Phys. Rev.* **D34**, 2739 (1986).
20. X.N. Wang and M. Gyulassy, *Phys. Rev. Lett.* **68**, 1480 (1992); X.N. Wang, *Phys. Rev.* **C58**, 2321 (1998)
21. M. Gyulassy et al., (2003) [nucl-th/0302077].
22. X.-N. Wang, (2004) [nucl-th/0412051].
23. V. Greco et al., *Phys. Rev. Lett.* **90**, 202302 (2003) and *Phys. Rev.* **C68**, 034904 (2003).
24. R. C. Hwa and C.B. Yang, *Phys. Rev.* **C70** 024905 (2004), and *J. Phys.* **G30** (2004) S1117-S1120.

25. R. Fries *et al.*, nucl-th/0407102 (2004).
26. N. Armesto *et al.*, (2004) [hep-ph/0411341]
27. H Stöcker, *Nucl. Phys.* **A750** (2005) 121.
28. H Stöcker, (2005) [nucl-th/0412022].
29. J. Casalderrey-Solana *et al.*, (2004) [hep-ph/0411315].
30. J. Ruppert and B. Müller, (2005) [hep-ph/0503158].
31. A. Majumder, *et al.* nucl-th/0412061.
32. K. Adcox *et al.*, *Nucl. Instrum. Meth.* **A499** (2003) 469.
33. J. Mitchell *et al.*, *Nucl. Instrum. Meth.* **A482** (2002) 491.
34. K. Adcox *et al.*, *Phys. Rev.* **C69** (2004) 024904.
35. N.N. Ajitanand *et al.*, *Nucl. Phys.* **A715** (2003) 765.
36. M. Chiu *et al.*, *Nucl. Phys.* **A715** (2003) 761.
37. C. Adler *et al.*, *Phys. Rev. Lett.* **90** 032301 (2003).
38. P. Stankus, *PHENIX Technical Note* **412** (2005).
39. N.N. Ajitanand *et al.*, (2005) [nucl-ex/0501025], submitted for publication.
40. S.S. Adler *et al.*, *Phys. Rev. Lett.* **91** 182301 (2003).
41. S.S. Adler *et al.*, (2004) [nucl-th/0411040]
42. A.M. Poskanzer *et al.*, *Phys. Rev.* **C58** (1998) 1671.
43. J. Bielcikova, S. Esumi, K. Filimonov, S. Voloshin, and J.P. Wurm, *Phys. Rev.* **C69** (2004) 021901.